Detecting Ecological Changes with a Remote Sensing Based Ecological Index (RSEI) Produced Time Series and Change Vector Analysis

Hanqiu Xu [1],*, Yifan Wang [1], Huade Guan [2], Tingting Shi [1] and Xisheng Hu [1,3]

[1] College of Environment and Resources, Key Laboratory of Spatial Data Mining & Information Sharing of Ministry of Education, Institute of Remote Sensing Information Engineering, Fujian Provincial Key Laboratory of Remote Sensing of Soil Erosion, Fuzhou University, Fuzhou 350116, China; N170620007@fzu.edu.cn (Y.W.); m171110011@fzu.edu.cn (T.S.); xshu@fafu.edu.cn (X.H.)

[2] National Centre for Groundwater Research and Training, College of Science and Engineering, Flinders University, Adelaide, SA 5001, Australia; huade.guan@flinders.edu.au

[3] College of Transportation and Civil Engineering, Fujian Agriculture and Forestry University, Fuzhou 350002, China

* Correspondence: hxu@fzu.edu.cn; Tel.: +86-591-2286-6071

Abstract: Increasing human activities have caused significant global ecosystem disturbances at various scales. There is an increasing need for effective techniques to quantify and detect ecological changes. Remote sensing can serve as a measurement surrogate of spatial changes in ecological conditions. This study has improved a newly-proposed remote sensing based ecological index (RSEI) with a sharpened land surface temperature image and then used the improved index to produce the time series of ecological-status images. The Mann–Kendall test and Theil–Sen estimator were employed to evaluate the significance of the trend of the RSEI time series and the direction of change. The change vector analysis (CVA) was employed to detect ecological changes based on the image series. This RSEI-CVA approach was applied to Fujian province, China to quantify and detect the ecological changes of the province in a period from 2002 to 2017 using Moderate Resolution Imaging Spectroradiometer (MODIS) data. The result shows that the RSEI-CVA method can effectively quantify and detect spatiotemporal changes in ecological conditions of the province, which reveals an ecological improvement in the province during the study period. This is indicated by the rise of mean RSEI scores from 0.794 to 0.852 due to an increase in forest area by 7078 km^2. Nevertheless, CVA-based change detection has detected ecological declines in the eastern coastal areas of the province. This study shows that the RSEI-CVA approach would serve as a prototype method to quantify and detect ecological changes and hence promote ecological change detection at various scales.

1. Introduction

Today, the world ecosystems are confronted with the problems of anthropogenic disturbances and resultant environmental variations more than ever before [1]. Increasing human activities have led to a significant increase in built areas on natural landscapes, causing substantial ecosystem disturbances at various scales [2]. Large-scale ecosystem disturbances have considerable influences on the global carbon cycle [3] and can exacerbate global climate change. The human-induced ecological disturbances exist over different ranges in terms of distances, magnitudes, and durations [4] and thus should be

monitored and quantified effectively. There is an increasing need for models to detect the spatial and temporal variation of ecological status.

Recent advances in remote sensing technology have provided a large amount of land surface data for ecosystem monitoring and a robust indication of ecological conditions at different scales [5,6]. Remote sensing imagery can be used to detect ecological status in various ranges because it measures reflected radiation of the Earth's surface and hence can detect different components of an ecosystem such as soil, vegetation and open water [7–9]. Therefore, remote sensing technology has been frequently utilized in ecosystem investigations [10–12]. In China, a remote sensing-assisted ecological assessment project has been performed nationwide for a period from 2000 to 2010 [13]. Similar studies have also been carried out in the United States protected areas [6] and other regions of the world [7,10,14].

A number of remote sensing indices have been created to quantify ecological status. Among them is the normalized difference vegetation index (NDVI) of Rouse et al. (1973) [15], which is the most widely utilized single indicator adopted in a variety of ecological studies [16–18]. Ivits et al. (2011) suggested that seasonal characteristics of vegetation cover derived from SPOT NDVI data could facilitate the monitoring of the suitability of farmland bird habitats [19]. The enhanced vegetation index (EVI) is another frequently used vegetation index. Alcaraz-Segura et al. (2017) demonstrated the use of EVI-derived Ecosystem Functional Attributes (EFAs) as predictors for Species Distribution Models (SDMs) by offering an early and integrative response of vegetation performance to environmental drivers. The study showed that EVI-derived EFAs could be used as meaningful essential biodiversity variables in SDMs [20]. Other single ecological indices have also performed as good ecological indicators. Ivits et al. (2009) developed the permanent vegetation fraction (PVF) to detect the unfavorable and favorable ecological conditions of the riparian zones in Spain [10]. A hyperspectral flower index (HFI) was designed to investigate flower phenology and flowering status in the Tibetan Plateau [21]. Caccamo et al. (2011) assessed the sensitivity of several spectral indices to drought in forests with Moderate Resolution Imaging Spectroradiometer (MODIS) products and found that the band 6-based infrared index had the highest sensitivity to drought intensity [14]. Land surface temperature (LST) retrieved from remote sensing thermal imagery has also been widely used to investigate regional thermal environments and was found to be reliable in evaluating urban heat island effect [22–26].

Aggregated remote sensing based ecological indices have advantages over single ones, as the aggregated index monitors ecological status with two or more metrics and thus can be used in the identification of more features related to ecological status. Tiner (2004) developed an aggregated index that integrated habitat disturbance and habitat extent indices to produce an overall numeric value for the natural habitat of a watershed [27]. The frequently-used forest disturbance index (DI) is also an aggregated index that combines three components of tasseled cap transformation of remote sensing data [28]. The MODIS global disturbance index (MGDI) proposed to map large-scale, regular disturbance of wildfire is an aggregation of MODIS Enhanced Vegetation Index (EVI) and LST products [29]. Rhee et al. (2010) used three indicators (LST, NDVI and the precipitation data of Tropical Rainfall Measuring Mission satellite) to develop the scaled drought condition index (SDCI). The three indicators were combined to form the index with selected weights [30]. The ecological niche modeling (ENM) method used to investigate bellbird seasonal migration patterns was developed by using three remote sensing indices (red index, EVI, and normalized difference water index) [31]. Gonçalves et al. (2016) combined SDMs with remote sensing metrics of vegetation and the predictors related to landscape structure, soils, and wildfires to analyse inter-annual habitat suitability dynamics. The results showed that coupling SDMs with remote sensing metrics might provide early-warnings of future changes potentially impacting habitat suitability [32].

Even though satellite remote sensing indices were frequently used to make spatially-explicit evaluations of regional ecological conditions, the remote sensing based ecological change detection remains a challenge due to the lack of the images showing comprehensive regional ecological status [33]. Although the existing indices can provide ecologically-related images, they are usually oriented to a

certain ecological-related theme (such as NDVI) and thus are not comprehensive ecologically-related images. A recent effort with an aggregated index, referred to as remote sensing based ecological index (RSEI) [12,34], has shown promise. The RSEI encompasses four indicators representing climatic and land-surface biophysical variables. The index has been successfully applied to many areas to reveal the comprehensive ecological status of the areas [35–39]. This study aims to use RSEI to produce time series of comprehensive ecological-status images for the Fujian province of China and employ change vector analysis (CVA) to detect the ecological change of the province based on the time series of the images. The RSEI-CVA approach will facilitate quick and effective quantification and detection of regional ecological changes over time and move one step towards the possibility to make the technique a relatively simple ecological change detection tool at various scales.

2. Study Area

The study area is Fujian province, located in the coastal zonal area of southeastern China (115°50′–120°40′E, 23°33′–28°20′N) (Figure 1). It faces the Taiwan Strait to the east. The terrain of Fujian is mostly mountainous. Fujian's forest ecosystem plays an important ecological role in China because it has the highest forest coverage rate (65.95%) among China's provinces (http://www.stats-fj.gov.cn/xxgk/ndsj). Fujian has a subtropical climate. The temperatures average around 6–10 °C in January but are higher in summer. Extreme temperature can be over 40 °C. The average annual precipitation is 1300–2000 millimeters (https://rp5.ru). Fujian has a terrestrial area of 122,017 km² and, as of the 2017 census, a population of 39.11 million. The province is divided into nine prefecture-level cities: Fuzhou, Xiamen, Quanzhou, Zhangzhou, Putian, Ningde, Sanming, Nanping, and Longyan.
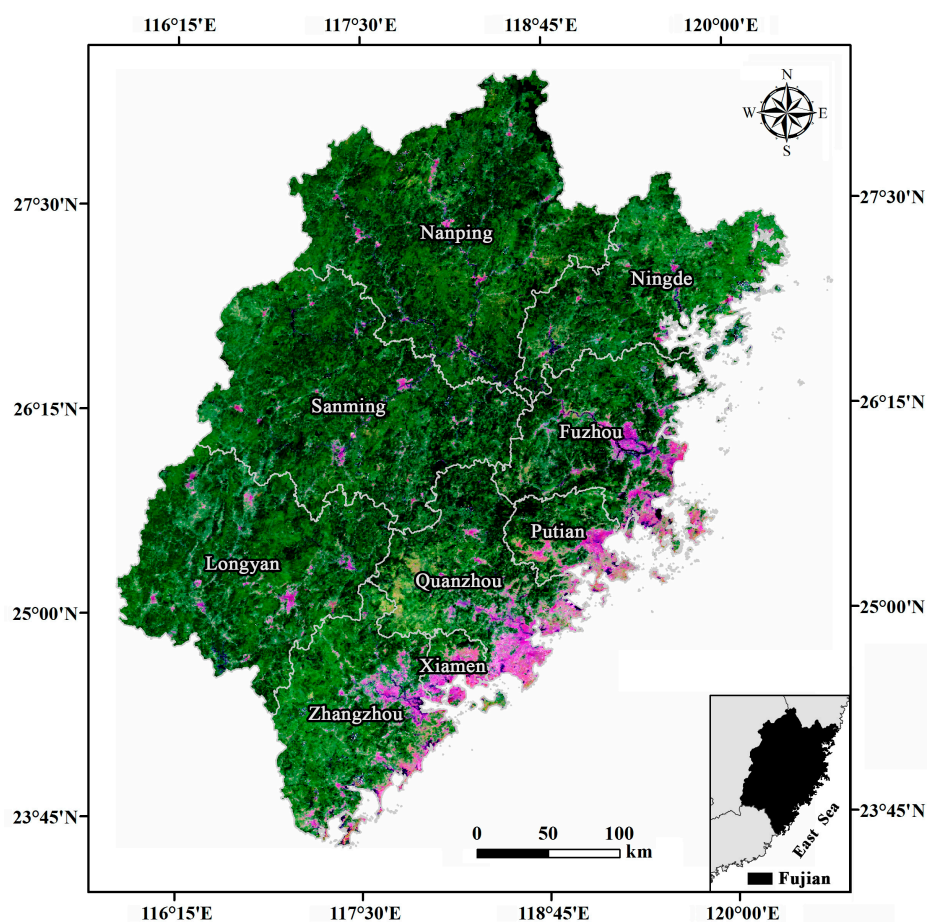

Figure 1. Location map of Fujian province and nine prefecture-level cities (2017 MODIS image).

Like many coastal Chinese provinces, the economic development of Fujian has been accompanied by a large influx of population, and much of the farmland has given way to impervious built-up areas. Therefore, Fujian is a suitable province for quantifying and detecting ecological changes.

3. Methods

3.1. Satellite Data

Routinely available MODIS data provides an effective way to observe and monitor ecological status over large scales and at regular intervals. In this study, we employed MODIS multitemporal 8-day surface reflectance composites (MOD09A1) and daily/8-day LST product (MOD11A1, MOD11A2) for the study period from 2002 to 2017. MODIS 500 m resolution surface reflectance composite has seven visible to mid-infrared bands. The product has been corrected for atmospheric effects such as aerosols, gasses, and Rayleigh scattering [40]. The 8-day MOD11A2 LST product provides per-pixel LST averaged from all the corresponding daily MOD11A1 LST pixels collected within that 8-day period [41].

To avoid temporal/seasonal variation effect that may cause different spectral responses, we selected the scenes only from those in the same month in leaf-on seasons. In spite of high-revisiting frequency, MODIS data still has a large number of missing observations in the rainy and cloudy subtropical areas like Fujian. As a result, only products in the September months of 2002, 2004, 2007, 2009, 2011, 2013, 2015 and 2017 meet the requirement and were used for the study at a 15-year interval. The scenes of the above products were downloaded from the NASA website (https://ladsweb.modaps.eosdis.nasa.gov). The study area was within a single MODIS tile.

The downloaded scenes were re-projected to the Universal Transverse Mercator (UTM) coordinate system using nearest neighbor resampling. The 16-bit reflectance data were converted to real values with the scaling factor of 0.0001, while the 16-bit LST data were converted to Kelvin values using the scaling factor of 0.02.

3.2. RSEI Ecological Index

3.2.1. Indicators Used in RSEI

RSEI is a newly developed aggregated index to fast detect ecological conditions solely using remotely sensed data [12]. The new aspects of the method are its consideration of four ecological indicators under the conceptual framework of pressure-state-response (PSR) to construct the model and application of Principal Components Analysis to integrate the four indicators.

The four indicators involved in RSEI are greenness (representing vegetation), moisture (representing soil moisture), heat (representing temperature), and dryness (representing built area), which are often involved in assessing ecological status as the four indicators are strongly correlated to ecological status and can be directly perceived by people [16,22]. The concept behind RSEI is such that any ecological changes will have a significant alteration in these four important characteristics of land surfaces. Accordingly, RSEI can be expressed as a function of the four indicators:

$$RSEI = f(Moisture, Greenness, Dryness, Heat) \tag{1}$$

Greenness is denoted with NDVI, which is the most commonly used vegetation index in measuring vegetation productivity due to its simplicity and robustness [16] and thus has long been used as a dominant ecosystem proxy variable [7]. The NDVI is expressed as [15]:

$$NDVI = (NIR - Red)/(NIR + Red) \tag{2}$$

where *NIR* and *Red* are the near-infrared (NIR1) and red bands of the MODIS 8-day reflectance image (MOD09A1), respectively.

Moisture was calculated by the wet component of a Tasseled Cap Transformation to represent soil moisture as the component was designed to understand important attributes of soil and plant moistures [42,43]. Soil moisture status was found to be the primary characteristic expressed in the wet component [44]. The wet component of MODIS data can be calculated as [45]:

$$Wet = 0.1147B1 + 0.2489B2 + 0.2408B3 + 0.3132B4 - 0.3122B5 - 0.6416B6 - 0.5087B7 \tag{3}$$

where $B1$ to $B7$ denote bands 1 to 7 corresponding to the *red*, *NIR*1, *blue*, *green*, *NIR*2, short-wavelength infrared 1 (*SWIR*1), and *SWIR*2 bands of the MODIS image, respectively.

Dryness is referred to as built-induced land-surface desiccation and thus can be represented by the index-based built-up index (IBI) [46]. The ecological status is affected greatly by human activities. The negative result is the conversion of natural landscapes to impervious built land and thus caused the dryness of land surface. The IBI can enhance built land and thus was selected. The index is expressed as:

$$IBI = \frac{2SWIR/(SWIR + NIR) - [NIR/(NIR + Red) + Green/(Green + SWIR)]}{2SWIR/(SWIR + NIR) + [NIR/(NIR + Red) + Green/(Green + SWIR)]} \tag{4}$$

where *SWIR*, *NIR*, *Red*, and *Green* are the SWIR1, NIR1, Red and Green bands of the MODIS image.

Heat is represented by thermal sensor data and in this case, was represented by MODIS LST product data. LST is an important metric frequently used to investigate ecological processes and climate change, as well as to study drought, evapotranspiration, vegetation density and surface energy balance [30,47,48].

3.2.2. Integration of the Indicators

Instead of using a traditional weighted sum approach, this study utilized a principal component analysis (PCA) method to combine the four metrics to form RSEI and selected the first component of PCA (PC1) to represent RSEI because PC1 explicates more than 76% of the total variation of the dataset (see Table 1 in the next section). The importance of each metric to RSEI is weighted by its loading to PC1. This prevents a subjective selection of weights for the metrics, which is usually done in the weighted sum method [30,49]. Accordingly, initial RSEI, $RSEI_0$, is represented by PC1:

$$RSEI_0 = PC1[f(Wet, NDVI, IBI, LST)] \tag{5}$$

The four metrics can be composited into a four-band image and then calculate using the covariance matrix for PC1 with image analyzing software using PCA function (such as ENVI, MATLAB, etc.). The values of the four metrics should be normalized between 0 and 1 before the performance of PCA because the data range and unit of the four metrics are different.

If the $RSEI_0$, i.e., PC1, has low values for good ecological conditions and high values representing poor ones, the $RSEI_0$ would be subtracted from one to let higher values represent better ecological status as usually expected:

$$RSEI = 1 - RSEI_0 = 1 - PC1[f(Wet, NDVI, LST, IBI)] \tag{6}$$

As such, the final RSEI has higher positive values indicating a greater likelihood of good ecological conditions.

RSEI was further normalized between 0 and 1. This procedure puts the scores for RSEI on a common scale between 0 and 1 for easy comparison with 1 denoting perfect ecological status and 0 indicating extremely poor one. The normalized RSEI was subdivided into five levels comparable with those of the Ecological Index (EI) to be described later. The divided five levels are Level 1 (0–0.2): very poor, Level 2 (0.2–0.4): poor, Level 3 (0.4–0.6): acceptable, Level 4 (0.6–0.8): good and Level 5 (0.8–1): very good [12,38,49].

Table 1. Contributions/loadings of four variables to the first principal component (PC1).

	2002 PC1	2004 PC1	2007 PC1	2009 PC1	2011 PC1	2013 PC1	2015 PC1	2017 PC1
Loading of Wet	−0.343	−0.278	−0.283	−0.522	−0.319	−0.444	−0.224	−0.308
Loading of NDVI	−0.810	−0.906	−0.851	−0.626	−0.816	−0.777	−0.848	−0.825
Loading of IBI	0.334	0.220	0.305	0.402	0.326	0.470	0.303	0.332
Loading of LST	0.340	0.231	0.320	0.416	0.355	0.498	0.373	0.338
Percent covariance eigenvalue (%)	78.26	81.08	78.36	80.01	79.33	83.33	76.83	86.36

Note: Loadings of NDVI and Wet in Table 1 have a negative sign in PC1, causing PC1, i.e., $RSEI_0$, has low values for good ecological condition and high values for poor one, as previously explained. A later subtraction of PC1 from 1 (Equation (6)) will make a conversion, i.e., NDVI and Wet will have a positive sign to PC1.

Such composed RSEI can be utilized to detect ecological status. In terms of RSEI's indicators, the most desirable ecological conditions would generally have higher vegetation coverage, higher soil-plant moisture, lower summer temperature and less land surface dryness [50,51]. The very poor ecological conditions may occur mainly in the deserts and intense soil-erosion areas with almost no vegetation and extremely hot and dry conditions [36,52,53]. Figure 2 illustrates the processing for RSEI.
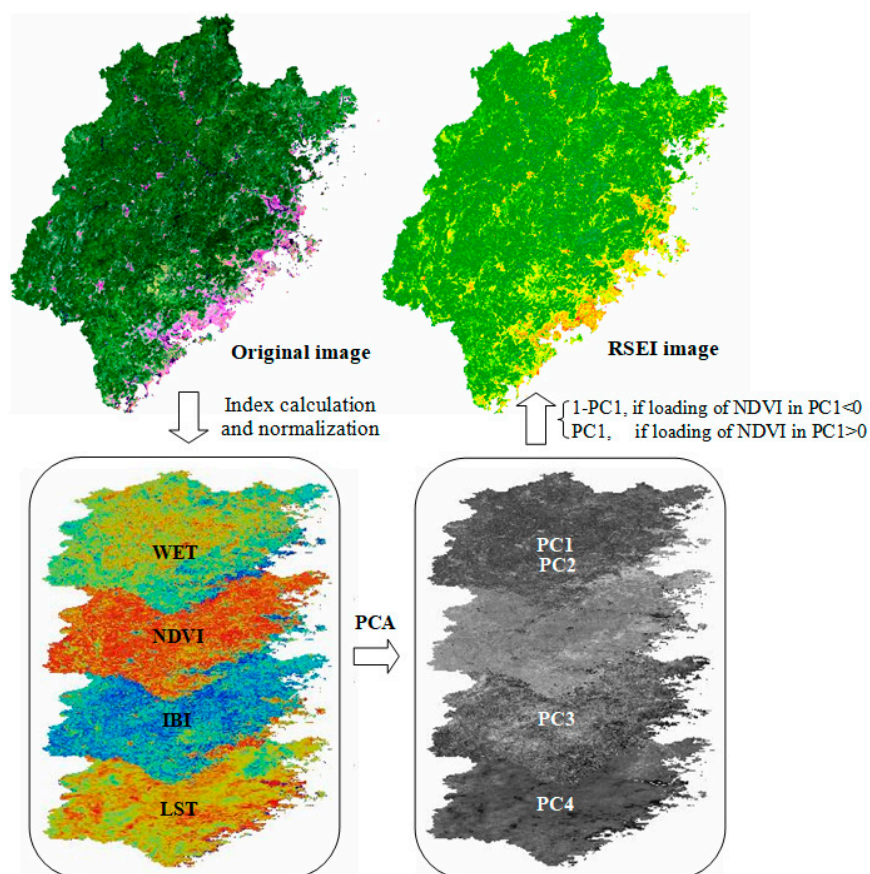
Figure 2. Sketch showing the processing for remote sensing based ecological index (RSEI).

For producing an RSEI time series, the computation of RSEI may have two ways. One is computing each year's RSEI directly using the original loadings of the four indicators of the corresponding year (see Table 1 in the next section). The other is calculating each year's RSEI with a set of fixed loadings that are averaged from the original loadings of per indicator in Table 1 across all study years (hereafter referred to as aRSEI). This is to remove fluctuations in resultant RSEI in case of the occurrence of abnormal loadings.

3.2.3. Improvement of RSEI

The LST indicator of RSEI in this study was represented by MODIS 1000 m resolution LST product, while the other three indicators have 500 m resolution as they were derived from 500 m resolution bands of MODIS data. The combination of a 1000 m resolution image with three 500 m resolution images will certainly lower the resolution of the resultant RSEI image and decline the ability of RSEI in differentiating spatial details of ecological status as the 1000 m LST image may average out important spatial heterogeneity of thermal features. Therefore, bias can result from a lumped representation of ecological processes especially in topographically complex terrain [54]. Successful downscaling of LST imagery to high spatial resolution would be crucial for modeling finer-scale ecological conditions and understanding complex patterns of ecological status. Therefore, the RSEI needs to be improved with a downscaled LST image that has a consistent resolution with the other three indicators.

A frequently used algorithm, TsHARP [55], was used to downscale the 1000 m LST imagery. TsHARP sharpened 1000 m LST imagery based on the regression-derived relationship between LST and NDVI that was derived from 500 m resolution red and near-infrared bands. Consequently, the 1000 m resolution LST image was sharpened to 500 m one. The main equation is expressed as (more details regarding the TsHARP method can be found in [55]):

$$f(NDVI) = a_0 + a_1 (1 - NDVI)^{0.625} \tag{7}$$

where $f(NDVI)$ is the function of NDVI aggregated to the 1000 m LST image, a_0 and a_1 are the parameters derived from the regression between the NDVI and LST.

The sharpened 500 m LST image was then combined with the three other indicators' 500 m images to produce a real 500 m resolution RSEI image.

3.2.4. Detecting Ecological Changes

The change vector analysis (CVA) was employed to detect ecological changes over the 15-year study period in Fujian. The CVA has been frequently used to reveal land cover dynamics [56–58]. It can detect changes occurring in the images between two different years. The CVA was conducted by computing the change vector (CV) between vectors **P** and **Q** using the RSEI image as well as the four indicators' images in years y_1 and y_2:

$$P = \begin{bmatrix} p_1 \\ p_2 \\ \vdots \\ p_n \end{bmatrix}, Q = \begin{bmatrix} q_1 \\ q_2 \\ \vdots \\ q_n \end{bmatrix} \tag{8}$$

where n is the number of indicators or the number of RSEI levels.

A change vector, ΔV, was then calculated:

$$\Delta V = P - Q = \begin{bmatrix} p_1 - q_1 \\ p_2 - q_2 \\ \vdots \\ p_n - q_n \end{bmatrix} \tag{9}$$

The change magnitude, $\|\Delta V\|$, was computed using the formula:

$$\|\Delta V\| = \sqrt{(p_1 - q_1)^2 + (p_2 - q_2)^2 + \cdots + (p_n - q_n)^2} \tag{10}$$

where $\|\Delta V\|$ denotes the total changes between **P** and **Q**. The greater the $\|\Delta V\|$, the higher the possibility of change.

A multi-threshold approach was applied to identify changes in the indicators. Thresholds can be determined as follows [56,57]:

$$CV_j(x,y) = \begin{cases} \text{change} & \text{if } |\Delta V_j(x,y)| \geq |\overline{V_j}| + \alpha_j \sigma_j \\ \text{no} - \text{change} & \text{if } |\Delta V_j(x,y)| < |\overline{V_j}| + \alpha_j \sigma_j \end{cases} \tag{11}$$

where $|\overline{V_j}|$ is the mean of the CV_j for the indicator j, σ_j is the standard deviation of the CV_j, and α_j is an adjustable parameter, which typically ranges from 0.0 to 1.5 [59]. In this study, the α_j we used for the multi-threshold approach ranges from 0.09 to 0.20, as suggested in [56].

To understand the attributes of ecological changes, a simple image differencing method [60] was employed using the 5-leveled RSEI images with the formula:

$$\Delta RSEI = RSEI_{y2} - RSEI_{y1} \tag{12}$$

where $y2$ is the end year and $y1$ is the start year of a time period. The positive value of the differencing result suggests an improvement in ecological condition, whereas the negative value indicates a decline.

3.2.5. Statistical Analysis

Statistical methods were used to analysis of RSEI results, including the Kolmogorov–Smirnov (K-S) test, Mann-Kendall (M-K) trend test and Theil-Sen (T-S) estimator.

K-S test [61]: The K-S test is a nonparametric method for comparing samples and was used to quantify a distance (D) between the empirical probability distribution functions of two samples (in this study case, two years) as it is sensitive to differences in both location and shape of the empirical cumulative distribution functions (ECDF) of the two samples. The D is defined as:

$$D_{m,n} = \sup_{RSEI} |F_{1,m}(RSEI) - F_{2,n}(RSEI)| \tag{13}$$

where $F_{1,m}(RSEI)$ and $F_{2,n}(RSEI)$ are the distribution functions of RSEIs of the first and the second year, respectively, sup is the supremum function, and m and n are the sample sizes of RSEIs of the first and the second year, respectively.

Values of D closer to zero indicate that the RSEI distributions in the two years are similar, whereas higher D values indicate a greater difference between the RSEI distributions in the two years. The null hypothesis of the K-S test is that samples have the same distribution, which can be rejected at the significance level α if

$$D_{m,n} > c(\alpha) \sqrt{\frac{m+n}{mn}} \tag{14}$$

The value of $c(\alpha)$ can be found from statistical books or calculated by:

$$c(\alpha) = \sqrt{-\frac{1}{2} \ln \alpha} \tag{15}$$

M-K trend test [62]: The test is used to examine data collected over time for consistently increasing or decreasing trends and therefore, can be used to determine whether an RSEI time series has a monotonic upward or downward trend. The following assumptions are made for the test: (1) the null hypothesis is that the RSEI time series to be detected has no monotonic trend, (2) the three alternative hypotheses are that a trend exists, which can be a positive, non-null, or negative trend.

For an RSEI time series $RSEI_1, RSEI_2, \ldots, RSEI_n$ ($n < 10$), the M-K statistic, S, was calculated as:

$$S = \sum_{i=1}^{n-1} \sum_{j=i+1}^{n} \text{sgn}(RSEI_j - RSEI_i) \tag{16}$$

where n is the number of the study years and is 8 in this case, $RSEI_i$ and $RSEI_j$ are the mean values of $RSEI$ of years i and j ($j > i$), respectively and sgn($RSEI_j - RSEI_i$) is the sign function as

$$\text{sgn}\left(RSEI_j - RSEI_i\right) = \begin{cases} +1, & \text{if } RSEI_j - RSEI_i > 0 \\ 0, & \text{if } RSEI_j - RSEI_i = 0 \\ -1, & \text{if } RSEI_j - RSEI_i < 0 \end{cases} \tag{17}$$

Given a significance level α, if $|S| \geq S_{\alpha/2}$, the null hypothesis is rejected, and the RSEI time series is considered to have a significant trend. If $S > 0$ or $S < 0$, the time series is considered to have an upward or downward trend. If $S = 0$, the time series has no trend.

T-S estimator [63,64]: The T-S estimator is robust for linear regression. It selects the median slope among all lines through pairs of two-dimensional sample points. The method can be more precise for skewed data than ordinary linear regression and is a very useful nonparametric method for estimating a linear trend.

The slope can be estimated as follows:

$$\beta_{RSEI} = median\left\{\beta_{ij} | \beta_{ij} = \frac{RSEI_j - RSEI_i}{Y_j - Y_i}\right\} \tag{18}$$

where β_{RSEI} is the slope of $RSEI$ time series, $RSEI_i$ and $RSEI_j$ are the mean $RSEI$ in years Y_i and Y_j ($j > i$). β_{ij} is the slope between pairs of mean $RSEIs$ of years i and j. If $\beta_{RSEI} > 0$, it indicates that the RSEI time series has an upward trend, whereas if $\beta_{RSEI} < 0$, it indicates a downward trend for the time series.

With that slope, pass a line through each pair of ($RSEI_i$ and $RSEI_j$) values to obtain n intercepts and select the median of the intercepts to estimate the regression intercept. The intercept of the regression equation can be calculated by:

$$\gamma = median\{y - \beta_{RSEI}x\} \tag{19}$$

where γ is the intercept, y is the mean $RSEI$ of different years, and x is the corresponding year.

4. Results

4.1. Ecological Status

RSEIs of Fujian of the study years were computed by scoring the PC1 of the four indicators based on their contributions. Table 1 is the PCA analysis results. It shows that PC1 has the largest eigenvalue among the four PCs in the study years, with a proportion ranging from 76% to 87%, indicating that PC1 gathers most variability information of the four metrics, compared with PC2, PC3, and PC4 (Table S1). Therefore, the four indicator variables are represented by PC1.

It is found that the four metrics in PC1 are grouped into two categories based on their signs, NDVI and Wet in one category, LST and IBI in the other. The opposite signs of the two categories suggest that their contributions to ecological status are in opposite ways. Contrarily, the signs of the four metrics in PCs 2, 3 and 4 cannot be grouped logically (Table S1). It is this finding that funds the RSEI with the PC1 score.

Figures 3 and 4 are the boxplot and the empirical cumulative distribution function (ECDF) diagram illustrating the RSEIs' distributions of the study years. The K-S test reveals that all D values are greater than 0.0038 (the value of Equation (14) at $\alpha = 0.001$ level) (Table 2). This indicates that these tests are significant at the 99.9% confidence level for a rejection of the null hypothesis of an identical distribution of the RSEIs between the two compared years. Nevertheless, the D values are generally smaller, within [0.07, 0.35], suggesting that the distributions of RSEIs are comparable. It can be found that 50% of each year's RSEI data are greater than 0.8 according to the ECDF. In addition, the D values are strongly correlated with the differences of mean RSEI of the compared year pairs ($r = 0.848$, $p < 0.001$, Table 2), indicating that the mean of RSEI can represent the overall ecological status of each study year.

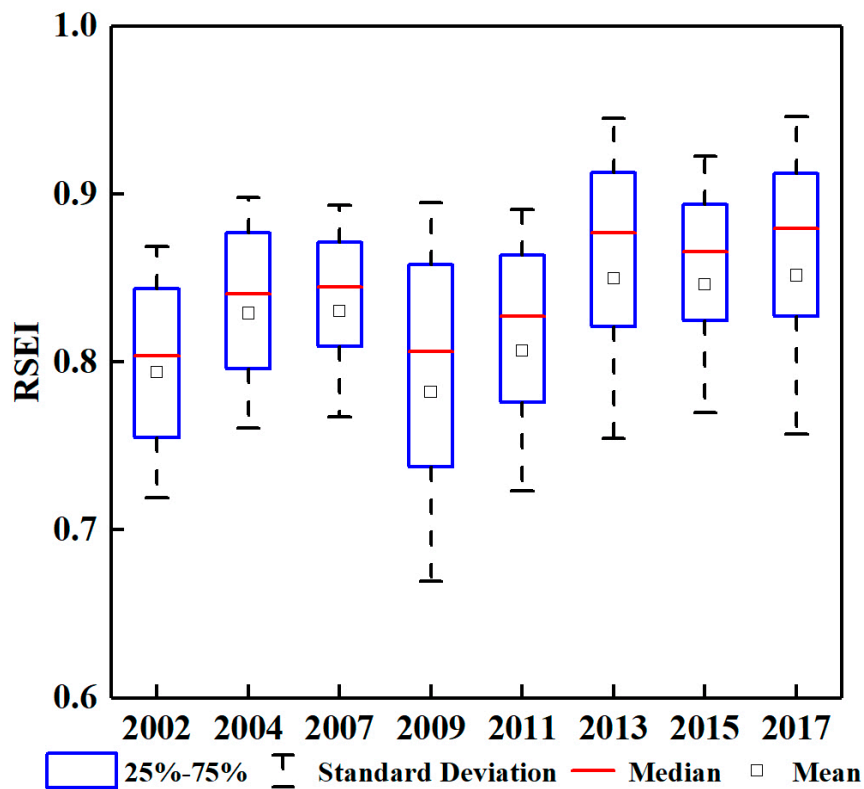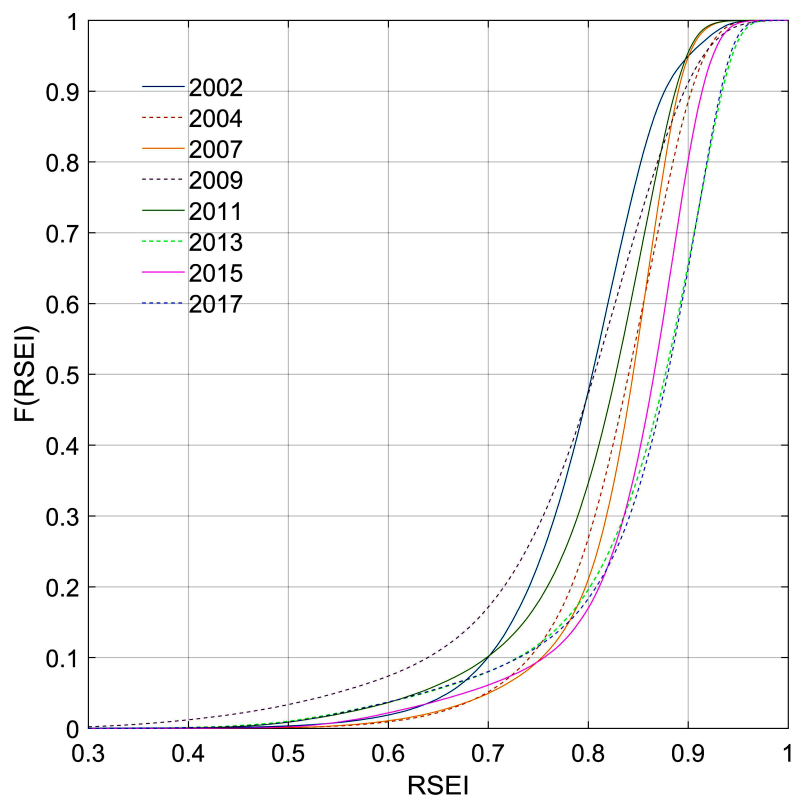**Figure 3.** Box plot showing the distribution of RSEI values in the study years.

Figure 4. Illustration of the empirical cumulative distribution functions (ECDF) of RSEI of each study year.

Table 2. The K-T test results.

Comparison Pair of Two Years	Difference of Mean RSEI in Absolute Value	*D* Value	*p* Value
2002 vs. 2004	0.0351	0.2371	0.0000
2004 vs. 2007	0.0011	0.0701	0.0000
2007 vs. 2009	0.0478	0.2663	0.0000
2009 vs. 2011	0.0243	0.1268	0.0000
2011 vs. 2013	0.0429	0.3500	0.0000
2013 vs. 2015	0.0041	0.1531	0.0000
2015 vs. 2017	0.0060	0.1574	0.0000

Table 3 is the statistics related to the RSEI images of the study years. The RSEIs were calculated using the original loadings (Table 1) rather than averaged loadings. This will be explained in detail in the Discussion section. Table 3 shows that the means of RSEI range from 0.782 to 0.852 (corresponding to Level 4 to Level 5). This indicates that the overall ecological quality of Fujian province during the study period was good to very good.

Table 3. Means of RSEI and four indicators.

Year	RSEI	Wet	NDVI	IBI	LST (k)
2002	0.794	−0.138	0.709	−0.227	300.74
2004	0.829	−0.120	0.726	−0.241	300.37
2007	0.830	−0.138	0.740	−0.244	301.02
2009	0.782	−0.139	0.693	−0.231	302.23
2011	0.807	−0.143	0.718	−0.242	301.92
2013	0.850	−0.119	0.735	−0.270	302.78
2015	0.846	−0.130	0.740	−0.258	299.41
2017	0.852	−0.134	0.756	−0.272	301.21

Table 3 also provides the means of the four indicators in the study period. NDVI that has the largest contribution (loading) to PC1 in all eight study years has increased by 0.047 (6.6%). Wet also increased by 2.9%, from −0.138 to −0.134. Of the two other indicators, IBI decreased by 19.8%, while LST increased by 0.5 k (0.2%). The increase of NDVI and Wet and the decrease of IBI can well counteract the slight increase of the LST factor and make an increment of RSEI by 7.3% in the study period. The four metrics of RSEI work together to produce a quantitative signal of the response to ecological stressors. The strength of RSEI not only lies in its final score for a particular area but also in the explanation of each of the four metric scores that represent specific spatial characterizations of ecological status. Therefore, RSEI, working as an aggregated index, is more holistic than its individual metrics.

Figure 5 is the RSEI images of the study years that comprehensively illustrate the ecological conditions of the province and their spatial variations in the study period. The reddish patches representing poor to very poor ecological condition areas scatter along with the eastern coastal zonal areas, which are relatively flat lowland areas in the province and hence have been intensively developed. The greenish patches denoting good to very good ecological conditions spread widely over areas of the province, where the topography is dominated by well-forested hills and mountains. The general greening trend indicates an improvement of the ecological condition of the province.
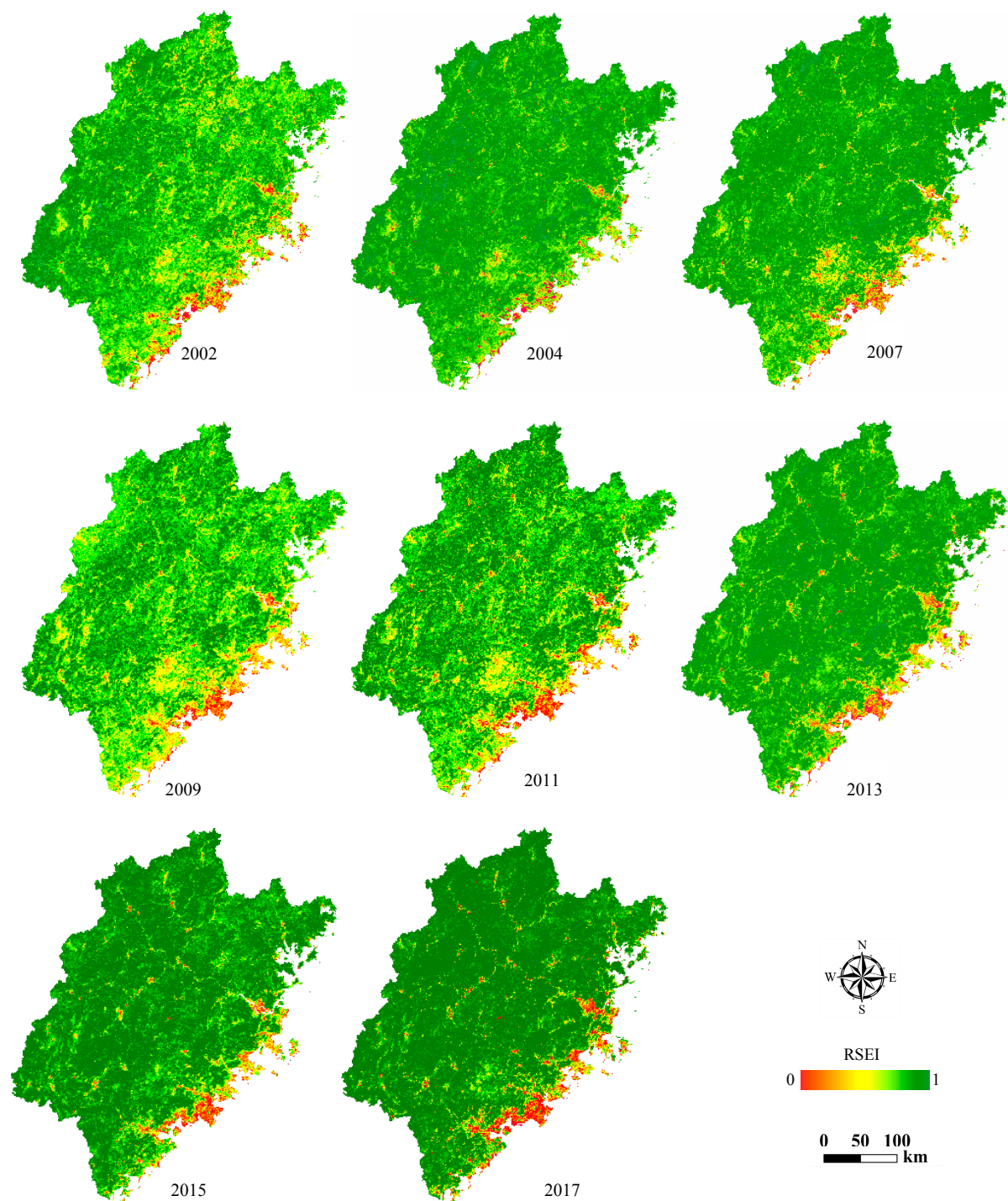
Figure 5. The time series of RSEI images showing the ecological status of Fujian province in each study year and the improvement of the overall ecological condition of Fujian during the study period.

The visible RSEI images make the index more understandable because the ecological status of a region is now characterized by numerous RSEI values rather than just one single numeric index value as provided by many traditional methods. As a result, the detailed ecological characteristics of each study year can be spatially identified and thus more comparable for change detection.

4.2. Spatiotemporal Ecological Changes

4.2.1. Temporal Change Analysis

Table 3 shows that the mean of RSEI has generally increased, up 7.3%, from 0.794 in 2002 to 0.852 in 2017. The M-K nonparametric test was used to verify if a trend existed in the RSEI time series. The test yields an S value of 16 ($n = 8$), which is greater than 14 (the value of $S_{\alpha/2}$ at the 0.05 significance level) and thus rejects the null hypothesis. Furthermore, the S value (16) is greater than 0, which indicates that the mean of RSEI has a significant upward trend from 2002 to 2017. The T-S estimator yields a linear regression model, $y = 0.0027x - 4.5942$. The slope value of 0.0027 is greater 0, also indicating an upward trend for the RSEI time series. In addition, the T-S estimator identifies 406098 pixels that have a significant positive trend in the study period, which is 4.13 times greater than the number of the pixels (79154) that have a negative significant trend (Table S2).

To detect changes between each study year, we divided each original RSEI images into five levels according to the interval described in Section 3.2.2 and then applied the CVA to the time series of the 5-leveled RSEI images. This reveals that the maximum change is at the interval of 2007–2009 as the ecological changed area reaches 43221 km^2 at the interval. This is followed by the intervals of 2009–2011 and 2002–2004 (Table 4, Figure 6a).

Table 4. Area statistics of ecological changes at each interval.

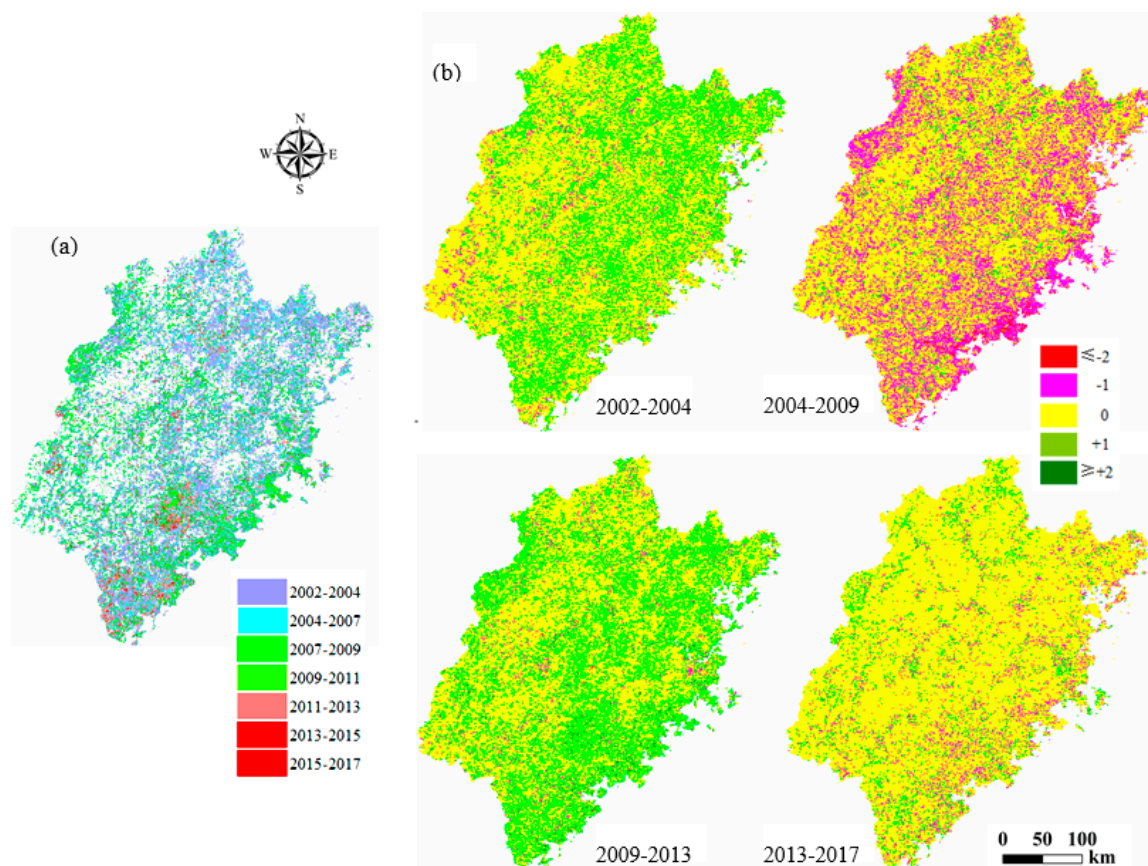|	2002–2004	2004–2007	2007–2009	2009–2011	2011–2013	2013–2015	2015–2017
Area (km^2)	34843	24892	43221	38042	27434	15893	16092

Figure 6. Change detection maps showing ecological status changes in various durations. (**a**) Time-series change detection mostly at a two-year interval, and (**b**) RSEI level-based change detection in four durations.

Figure 7 is a scatter plot showing the T-S regression-based temporal change trend of RSEIs in the study period and illustrating the segmentation of the sub-period of the study years from 2002 to 2017. According to the maximum distance of the scatter points to the trend line in each duration (blue bar) suggested in [65], the study period was divided into four change durations, which are 2002–2004, 2004–2009, 2009–2013 and 2013–2017 (indicated in dash lines in Figure 7).
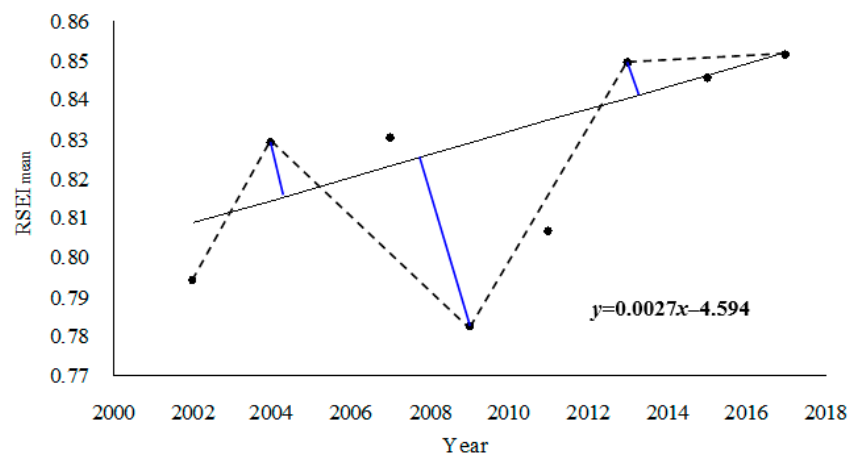

Figure 7. Temporal segmentation to detect ecological improvement and decline durations for the study period.

The image differencing approach [60] was implemented using the 5-leveled RSEI images to understand the attributes of the ecological change in each of the four durations. The positive value of the differencing result suggests an improvement in ecological conditions, while the negative value indicates a decline. Figure 6b is the level-change map ($\Delta RSEI$) of the four durations. Maps of durations 2002–2004 and 2009–2013 are distinguished by green patches, indicating improvements in ecological condition in the two durations, whereas duration 2004–2009 illustrates a great decline, suggested by a reddish appearance, as the RSEI values dropped by 6% in the duration (Table 3). Yellow patches dominate the duration of 2013–2017. This suggests no substantial difference in ecological conditions between the two years.

4.2.2. Spatial Change Analysis

The change magnitude ($\|\Delta V\|$) of the four indicators (Wet, NDVI, IBI, and LST) between 2002 and 2017 was first calculated. It well illustrates the spatial ecological changes (Figure 8). Figure 8a–c shows a high-magnitude ecological change area due to significant built-up land increases. Figure 8d–f shows a low-to-middle magnitude of ecological improvement due to the greening in former low forested areas. The whole CVA magnitude map of Fujian is presented in Figure 8g. It shows that the ecological changes in the study period mainly occurred in the east area of the dashed line running roughly from the north end to the south end of the province's territory. The high values of $\|\Delta V\|$, represented by reddish patches mainly appear in the coastal areas of the province, indicating that the areas have witnessed intensive ecological changes.
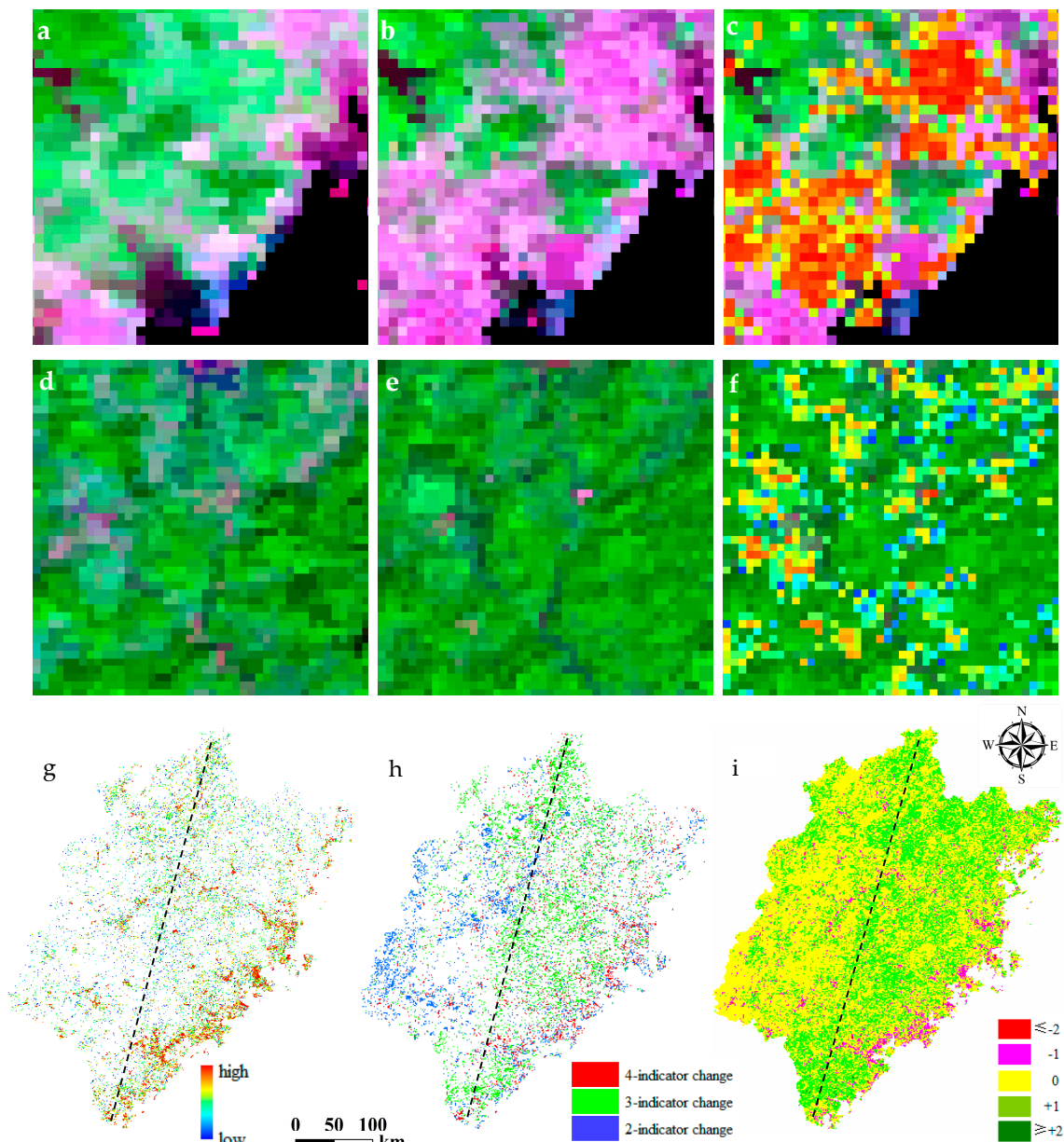
Figure 8. Ecological change maps in the 2002–2017 period. (**a**–**c**) Ecological change in a coastal area, (**d**–**f**) Ecological change in a forested area [(**a**,**d**) original images of 2002, (**b**,**e**) original images of 2017, (**c**,**f**) change maps, see Figure 8g for legend], (**g**) Change magnitude map of four indicators, (**h**) Change intensity map of four indicators and (**i**) Change attribute map of RSEI.

CVA was also calculated for each of the four RSEI's indicators. The change images of the four indicators were then overlaid to form a change intensity map (Figure 8h), in which the pixel that underwent changes in all four indicators were represented by red colour, suggesting an intensive change in that pixel. The green- and blue-cloured pixels denote the areas that had changes in three and two indicators, respectively (for the clarity of the map, the patches with one-indicator change are not shown in the figure). The red patches, accounting for 1.6% of the change area (Table 5), occur mainly in the eastern coastal areas. This again suggests the intensive ecological changes in the coastal areas.

Table 5. Statistics of change intensities and attributes in the period 2002–2017.

Change Intensity			Change Attribute		
Number of Indicator Change	Area (km^2)	Percentage (%)	Number of Level Change	Area (km^2)	Percentage (%)
4	2005.79	1.64	−4	1.76	
3	10397.35	8.52	−3	21.13	
2	7767.82	6.36	−2	323.05	5808.63 — 4.76
1	24827.98	20.36	−1	5462.68	
			0	77018.27	77018.27 — 63.12
			1	39030.57	
			2	157	39189.58 — 32.12
			3	2.01	

Image differencing between the 5-leveled RSEI images of 2002 and 2017 was further performed to reveal change attributes. Figure 8i is the change-attribute maps (Δ*RSEI*) of the period. The map highlights the spatial distribution of the attributes of the ecologically-changed areas in the period. The red-tone patches representing ecologically-declined areas also occur mainly in the coastal zonal areas, the greenish patches denoting ecologically-improved areas spread from northeast to southeast, whereas the west part of the province remains mostly unchanged (yellow colored). Area statistics reveal the level changes during the period (Table 5). A total area of 77,018 km^2 in Fujian remains unchanged in RSEI levels during the study period and thus suggests no change in ecological conditions, while the ecologically improved area (32.12%) is considerably greater than that of ecologically declined area (4.76%). This contributes to the ecological improvement of Fujian.

4.3. Comparison of RSEIs Computed with and without Sharpened LST

The RSEI used in this study has been improved with a sharpened LST image (hereafter referred to as RSEI-shp). The differences between the RSEI-shp and the RSEI without using a sharpened LST image (hereafter referred to as RSEI-nonshp) should be explored. Data in Table 6 indicates that RSEI-shp has a higher value (<5%) than RSEI-nonshp. Figure 9 shows that RSEI-nonshp, computed using a 1000 m LST image (Figure 9b) with three other indicators' 500 m images, misses some spatial details (Figure 9d). In contrast, RSEI-shp can pick up more spatial details when a sharpened 500 m LST image is used (Figure 9e), because there are significant differences in spatial details between the original 1000 m resolution LST image (Figure 9b) and the sharpened 500 m resolution LST image (Figure 9c) (one 1000 m-resolution pixel = four 500 m-resolution pixels).

Table 6. Comparison between RSEIs computed with and without sharpened LST.

	2002	2004	2007	2009	2011	2013	2015	2017
RSEI-nonshp	0.758	0.795	0.795	0.745	0.771	0.815	0.811	0.817
RSEI-shp	0.794	0.829	0.83	0.782	0.807	0.85	0.846	0.852
Percentage difference (%)	4.75	4.28	4.40	4.97	4.67	4.29	4.32	4.28

To quantitatively examine the effect of the sharpened LST on RSEI, we have tested the samples with different plant and built cover proportions that were identified by visual interpretation. The results clearly show a significant enhancement of RSEI value in built land (Figure 10). In high-density built area, sharpened LST can increase RSEI value by up to 62%. This is because the sharpened LST can help pick up fine vegetation patches that have a few pixels between large built patches and may otherwise be averaged out in a coarser-resolution LST image. The increasing rate is getting lower with the increase of vegetation proportion. There is almost no difference between sharpened and non-sharpened RSEIs in dense forest area (Figure 10), which can be visually examined at the northwestern corner of Figure 9d,e.
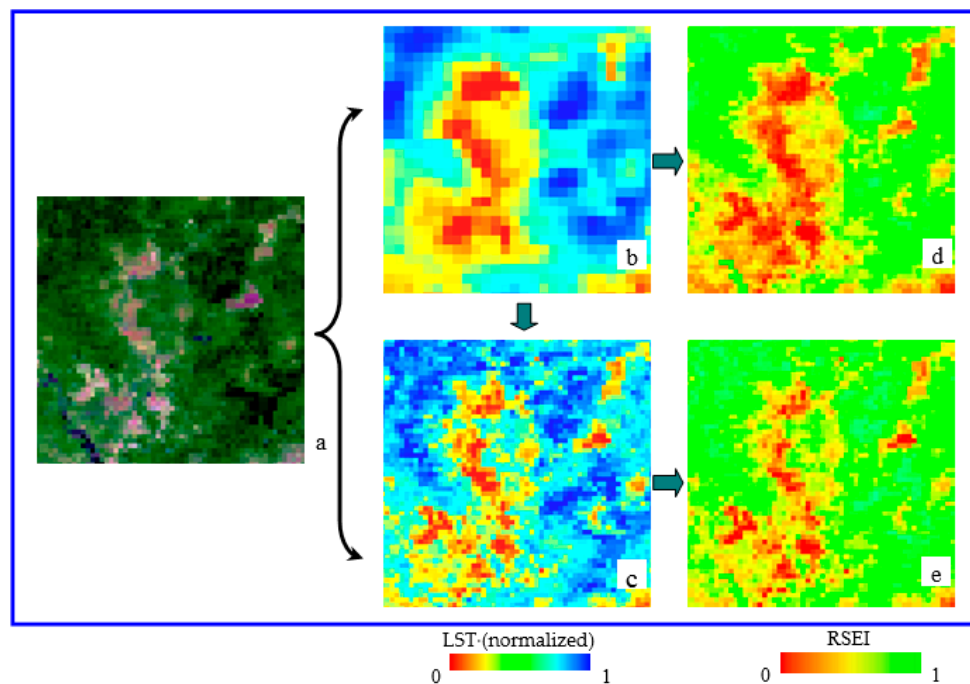
Figure 9. Comparison between RSEI-shp and RSEI-nonshp. (**a**) original image, (**b**) original 1000 m LST image, (**c**) sharpened 500 m LST image, (**d**) RSEI-nonshp image computed using the 1000 m LST image, (**e**) RSEI-shp image computed with the sharpened 500 m LST image.
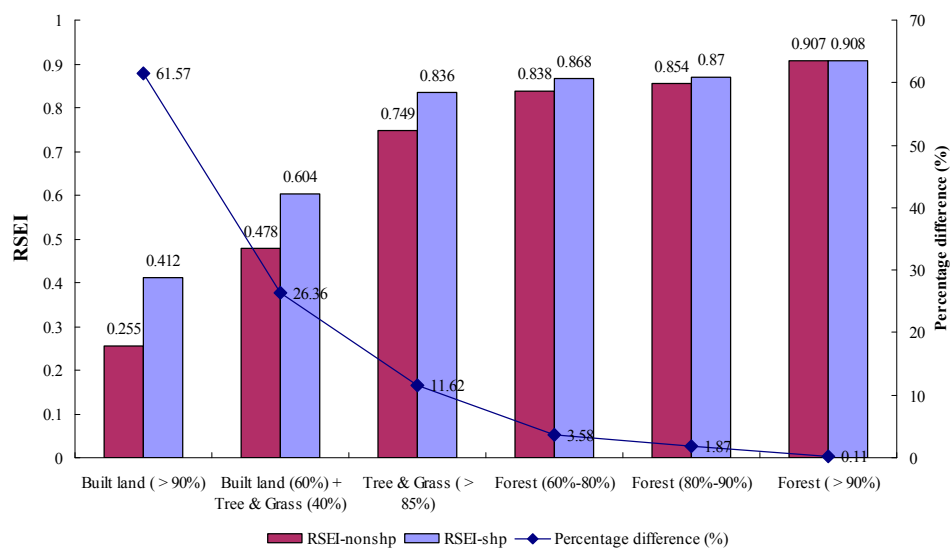

Figure 10. Comparison between RSEIs computed with and without sharpened LST in the samples with different proportions of built land and plant cover.

4.4. Comparison of RESI with Existing Ecological Indices

The Ecological index (EI) is currently used in China by the Ministry of Environmental Protection (MEP) of China [49] as an official index to evaluate annual ecological status for administrative divisions at the county level and above. The EI is aggregated with five indices (vegetation coverage, biological richness, water network density, pollution load and land stress) using a weighted sum method. EI is scored between 0 and 100 and also divided into five levels. Therefore, EI is comparable with RSEI. The details about the definition and calculation of each index can be found in [49].

In this study, the results of RSEI were compared with those of officially-announced EIs for Fujian (Table 7). The comparison was limited to the results after 2007 because the EI evaluation system started in 2006 and thus no EI value is available for 2002 and 2004.

Table 7. Comparison between EI and RSEI results.

		2007	2009	2011	2013	2015	2017
EI	value	83.2	82.2	81.1	82.3	82.4	81.3
	Level	5	5	5	5	5	5
RSEI	value	83.0	78.2	80.7	85.0	84.6	85.2
	Level	5	4	5	5	5	5

Note: RSEI values were multiplied by 100.

It can be found that the RSEI's results are mostly comparable with EI ones in either data value or ecological level though the two systems utilize different model factors. Although there is a level difference in 2009 between the two indices (EI is one level higher than RSEI), the value of RSEI (78.2) is close to the lower end of Level 5, suggesting no significant difference between them. Previous work in Guangdong [37,66] also had the same conclusion. Yue at al. (2019) have developed another ecological index that combines 17 indicators to evaluate ecological conditions in three cities, Beijing, Nanjing and Shanghai [38]. They also found the evaluation results were similar to those of RSEI.

The comparison of the results between RSEI and EI has demonstrated the similarity of the two indices. The differences between RSEI and EI lies in (1) EI provides the result only with a single numeric value, whereas RSEI provides not only the value, but also an ecological-status image that indicates spatial difference of regional ecological conditions and can be used for spatial and temporal change detections, (2) application of EI is limited to the administrative region not lower than county level because the data used to calculate EI are mainly based on annual official statistics books that are issued only for the administrative region at county level or above, while RSEI has no this limitation and hence can be applied to any areas, and (3) the computation of RSEI is easier and quicker than that of EI. It is generally expected to have a method that is simple but can characterize the entire ecosystem effectively and efficiently [67].

5. Discussion

The spatial and temporal change detection for a region's ecological status is a challenge due to the difficulty in producing the time series of ecological images showing comprehensive ecological status. To meet this requirement, we develop a prototype method by employing the remote sensing based ecological index, i.e., RSEI, associated with the multiple threshold CVA method. The RSEI technique makes distinctions among different ecological change related approaches because the result of the RSEI approach is not provided only with a single numeric value, but also a comprehensive ecological-status image that illustrates the spatial difference of regional ecological conditions. This ecological-status image will help to make change detections spatially and temporally, such as those demonstrated in this study. This otherwise would be difficult.

The development of RSEI is under the conceptual framework of pressure-state-response (PSR) which is one of the most frequently-used ecological environment related conceptual frameworks [34,35,68]. The PSR is rooted in the notion of causality [69–71] and built upon the selection of metrics for three classes: metrics of anthropogenic pressures (P), ecological environment states (S) and climate responses (R). For example, the selection of dryness indicator, represented by IBI, for RSEI is to signify human activity-induced pressures on the ecosystem. The greenness indicator, denoted by NDVI, was chosen as a metric to measure the ecological state before and after human-induced land surface changes. The indicators of ground surface moisture and heat were represented respectively by moisture and land surface temperature, which reveal climate changes responding to the state changes of the ecosystem.

The weighting method is an important process in the development of aggregated ecological indices. Multi-indicators were usually combined to form an aggregated index with a set of weights that were usually selected subjectively, such as the weights of MEP's EI [49] that have been argued since its issue [72,73]. Rhee et al. (2010) also provided three sets of weights to integrate three indicators for SDCI [30]. They pointed out that the SDCI would be improved if the weights for the three indicators were optimized. In order to avoid the impact of subjective experience on weight assignment, RSEI employed a covariance-based (unstandardized) PCA to find the importance of each involved indicator. The weight for each indicator is objectively and automatically assigned based on the load (contribution) of each indicator to PC1. This avoids the errors derived from the weight definition due to individual characteristics [34].

As far as the robustness of the index is concerned, RSEI has been widely used in regions with different landscapes. The application results have shown that RSEI can effectively distinguish ecological status from different landscapes. For example, RSEIs are usually within 0.45–0.61 in islands [74,75], 0.45–0.59 in cities [35,37,76–78], higher than 0.63 in forested/densely-vegetated regions [12,50,51], but can be as low as 0.18 in intense soil-erosion areas [36,75] and 0.24 in desert areas [53,79,80]. The applications of RSEI in different areas with various ecological conditions have suggested its robustness in evaluating area ecological status.

This study has revealed an improvement of ecological conditions in Fujian province from 2002 to 2017 in terms of RSEI-value raise. This is due largely to long-term afforestation, along with forest conservation (closing hillsides for tree growing), in the province (http://www.fjlgy.com/SView2011.aspx). A total of 7078 km^2 forested lands have increased during the period (Table S3). Although the built-up area also increased by 2996 km^2 in the period, the magnitude of the increase is much lower than that of the forest. Moreover, the contribution of vegetation to the PC1-based RSEI measurement is much higher than that of built-up land and is the highest among the four indicators (Table 1).

This study also found the difference in ecological change between eastern and western Fujian province as ecologically-declined areas mostly occurred in the eastern region. This is because the population density of the six prefecture-level cities in the eastern area is 3.7 times higher than that of the three prefecture-level cities in the western area (Figure 1). In addition, the GDP of the six eastern cities is 3.5 times higher than that of the three western cities (http://www.chyxx.com/industry/201901/710860.html). This suggests a much higher anthropogenic pressure on regional ecological status in the eastern province.

A notable RSEI change is the significant decline of RSEI in 2009. This is due partly to the difference in land cover type changes. The built-up area increased almost two times more than forest area in the duration of 2007–2009 (521 km^2 (built area) vs. 171 km^2 (forested area), Table S3). This greatly enhances the contribution (loading) of built-up lands (IBI) to RSEI from 0.305 to 0.402, lowers the contribution of forests (NDVI) from absolute values 0.851 to 0.626 (Table 1). The meteorological condition also affects the year's ecological conditions. The precipitation of 2009 is 183 mm lower than that of 2007 although the air temperature of 2009 was 0.17 °C slightly lower than that of 2007. The combinations of the four factors' interactions, therefore, results in a decline of RSEI. This 2009 case demonstrates that RSEI, as a four-indicator combined index, can correctively capture land cover and climatic variations and identify the most vital factor that influences regional ecological changes while counteracting the contribution of opposite factors.

This study has demonstrated that the RSEI can work well with MODIS data. This would facilitate large-scale detection of regional ecological changes over time. The change-detection maps of the RSEI time-series would be useful for the regional decision-makers for the prevention of degradative situations in the detected ecologically-declined areas, such as those marked in red color in Figure 8g–i.

In this study, we used original loadings instead of averaged loadings to produce each year's RSEI image. This is because the aRSEI time series, calculated using averaged loadings, do not reflect the ecological improvement of the study area. The loadings averaged from Table 1 are 0.340 for Wet, 0.807 for NDVI, −0.337 for IBI and −0.359 for LST. The averaged loading-produced result (Table S3) shows

almost no difference in the aRSEI scores between 2002 and 2017 (0.8429 vs. 0.8465). This means that the ecological status of the province remains almost no change in the period, even if the 7078 km^2 forests have been planted. Therefore, the aRSEI result is unable to explain the ecological improvement of Fujian province. This is because the average-loading method may weaken the effects of annual land surface and meteorological condition changes and thus causes very low correlations between aRSEI scores and the four factors that are the main factors causing ecological changes (Table S3 and Figure S1). Consequently, the ecological changes represented by aRSEI scores cannot be explained by any of the four factors. In contrast, the RSEI scores achieve much higher correlations to the four factors (Table S3, Figure S1), especially with forest, built land and precipitation factors as discussed previously. This means the ecological changes in the 15-year study period of Fujian province can be well interpreted by RSEI. In addition, the results of statistical tests (M-K trend test and T-S estimator) also show that RSEI outperforms aRSEI (Table S4). This makes RSEI more reliable for comparison across years than aRSEI. However, this may not always be the case with different applications (i.e., different areas and different imagery). The users may need to calculate both RSEI and aRSEI scores and choose the one that can better reflect ecological conditions and changes for their study areas.

The detected ecological change areas were checked visually in this study, as illustrated in Figure 8a–f. A quantitative ground truth may be somewhat difficult because RSEI is a combination of four indicators rather than based on a certain land cover. Therefore, the extent of ecological status change may not exactly follow that of the land cover change. For example, pixels that have been converted from vegetation to build land may have a clear boundary showing the change extent. However, the boundary of the resultant ecological change may not exactly follow the land-cover change boundary because this ground cover change may also affect the ecological conditions of adjacent pixels, causing the changes in heat and wetness conditions for the adjacent pixels.

6. Conclusions

Remote sensing is of value to a nearly continuous measurement of spatial distributions of ecological conditions and provides measurement metrics of the ecological processes. Nevertheless, remote sensing-based ecological status mapping and change detection remain challenging because of the difficulty in producing the time series of ecological images solely based on remote sensing data. This study has demonstrated that the improved RSEI with sharpened LST imagery can effectively quantify regional ecological status, and the RSEI-produced time series of ecological-status images can be useful for detection of long-term ecological changes with the assistance of the multiple threshold CVA approach.

The RSEI-CVA approach reveals the improvement of ecological conditions in Fujian province in the 15-year study period due largely to the great increase in forested land. This result is supported by those obtained with the EI index of MEP but is more meaningful. RSEI provides not only a single numeric value to describe an overall ecological condition as EI does, but also a visible ecological image that illustrates the location and extent of different ecological conditions. Such information is of great value for decision making process regarding management and restoration of regional ecological quality, such as forest cleaning practices, wildfire prevention campaigns, etc. Therefore, RSEI can work as a good surrogate to monitor regional ecological status. The RSEI-CVA technique would serve as a prototype method to quantify and detect ecological changes over time and hence promote ecological change detection at various scales.

The development of RSEI is aimed to assess general ecological status using four indicators that are strongly correlated to general ecological conditions. Therefore, it is not recommended to use the index for some special cases such as species–related habitat analysis or biodiversity study.

References

1. McDonnell, M.J.; MacGregor-Fors, I. The ecological future of cities. *Science* **2016**, *352*, 936–938. [CrossRef] [PubMed]

2. Williams, M.; Longstaff, B.; Buchanan, C.; Llanso, R.; Dennison, W. Development and evaluation of a spatially-explicit index of Chesapeake Bay health. *Mar. Pollut. Bull.* **2009**, *59*, 14–25. [CrossRef] [PubMed]

3. Baldocchi, D. Breathing of the terrestrial biosphere: Lessons learned from a global network of carbon dioxide flux measurement systems. *Aust. J. Bot.* **2008**, *56*, 1–26. [CrossRef]

4. Levin, S.A. The problem of pattern and scale in ecology: The Robert H. MacArthur Award Lecture. *Ecology* **1992**, *73*, 1943–1967. [CrossRef]

5. Qiu, B.W.; Chen, G.; Tang, Z.H.; Lu, D.F.; Wang, Z.Z.; Chen, C. Assessing the Three-North Shelter Forest Program in China by a novel framework for characterizing vegetation changes. *ISPRS J. Photogramm.* **2017**, *133*, 75–88. [CrossRef]

6. Willis, K.S. Remote sensing change detection for ecological monitoring in United States protected areas. *Biol. Conserv.* **2015**, *182*, 233–242. [CrossRef]

7. De Araujo Barbosa, C.C.; Atkinson, P.M.; Dearing, J.A. Remote sensing of ecosystem services: A systematic review. *Ecol. Indic.* **2015**, *52*, 430–443. [CrossRef]

8. Kwok, R. Ecology's remote-sensing revolution. *Nature* **2018**, *556*, 137–138. [CrossRef]

9. Reza, M.I.H.; Abdullah, S.A. Regional Index of Ecological Integrity: A need for sustainable management of natural resources. *Ecol. Indic.* **2011**, *11*, 220–229. [CrossRef]

10. Ivits, E.; Cherlet, M.; Mehl, W.; Sommer, S. Estimating the ecological status and change of riparian zones in Andalusia assessed by multi-temporal AVHHR datasets. *Ecol. Indic.* **2009**, *9*, 422–431. [CrossRef]

11. Kennedy, R.E.; Andréfouët, S.; Cohen, W.B.; Gómez, C.; Griffiths, P.; Hais, M.; Healey, S.P.; Helmer, E.H.; Hostert, P.; Lyons, M.B.; et al. Bringing an ecological view of change to Landsat-based remote sensing. *Front. Ecol. Environ.* **2014**, *12*, 339–346. [CrossRef]

12. Xu, H.Q.; Wang, M.Y.; Shi, T.T.; Guan, H.D.; Fang, C.Y.; Lin, Z.L. Prediction of ecological effects of potential population and impervious surface increases using a remote sensing based ecological index (RSEI). *Ecol. Indic.* **2018**, *93*, 730–740. [CrossRef]

13. Ouyang, Z.Y.; Wang, Q.; Zheng, H.; Zhang, F.; Hou, P. National ecosystem survey and assessment of China (2000–2010). *Bull. Chin. Acad. Sci.* **2014**, *29*, 462–466.

14. Caccamo, G.; Chisholm, L.A.; Bradstock, R.; Puotinen, M.L. Assessing the sensitivity of MODIS to monitor drought in high biomass ecosystems. *Remote Sens. Environ.* **2011**, *115*, 2626–2639. [CrossRef]

15. Rouse, J.W.; Haas, R.H.; Schell, J.A.; Deering, D.W. Monitoring vegetation systems in the Great Plains with ERTS. In Proceedings of the Third ERTS Symposium, NASA SP-351, Washington, DC, USA, 10–14 December 1973; pp. 309–317.

16. Mishra, N.B.; Crews, K.A.; Thoralf, N.M.; Kenneth, R.Y. MODIS derived vegetation greenness trends in African Savanna: Deconstructing and localizing the role of changing moisture availability, fire regime and anthropogenic impact. *Remote Sens. Environ.* **2015**, *169*, 192–204. [CrossRef]

17. White, D.C.; Lewis, M.M.; Green, G.; Gotch, T.B. A generalizable NDVI-based wetland delineation indicator for remote monitoring of groundwater flows in the Australian Great Artesian Basin. *Ecol. Indic.* **2016**, *60*, 1309–1320. [CrossRef]

18. Dubinin, V.; Svoray, T.; Dorman, M.; Perevolotsky, A. Detecting biodiversity refugia using remotely sensed data. *Landsc. Ecol.* **2018**, *33*, 1815–1830. [CrossRef]

19. Ivits, E.; Buchanan, G.; Olsvig-Whittaker, L.; Cherlet, M. European farmland bird distribution explained by remotely sensed phenological indices. *Environ. Model. Assess.* **2011**, *16*, 385–399. [CrossRef]

20. Alcaraz-Segura, D.; Lomba, A.; Sousa-Silva, R.; Nieto-Lugilde, D.; Alves, P.; Georges, D.; Vicente, J.R.; Honrado, J.P. Potential of satellite-derived ecosystem functional attributes to anticipate species range shifts. *Int. J. Appl. Earth Obs.* **2017**, *57*, 86–92. [CrossRef]

21. Chen, J.; Shen, M.; Zhu, X.; Tang, Y. Indicator of flower status derived from in situ hyperspectral measurement in an alpine meadow on the Tibetan Plateau. *Ecol. Indic.* **2009**, *9*, 818–823. [CrossRef]

22. Coutts, A.M.; Harris, R.J.; Phan, T.; Livesley, S.J.; Williams, N.S.G.; Tapper, N.J. Thermal infrared remote sensing of urban heat: Hotspots, vegetation, and an assessment of techniques for use in urban planning. *Remote Sens. Environ.* **2016**, *186*, 637–651. [CrossRef]

23. Estoque, R.C.; Murayama, Y. Monitoring surface urban heat island formation in a tropical mountain city using Landsat data (1987–2015). *ISPRS J. Photogramm.* **2017**, *133*, 18–29. [CrossRef]

24. Xu, H.Q.; Chen, B.Q. Remote sensing of the urban heat island and its changes in Xiamen City of SE China. *J. Environ. Sci.* **2004**, *16*, 276–281.

25. Xu, H.Q.; Hu, X.J.; Huade, G.; He, G.J. Development of a fine-scale discomfort index map and its application in measuring living environments using remotely-sensed thermal infrared imagery. *Energy Build.* **2017**, *150*, 598–607. [CrossRef]

26. Huang, G.; Cadenasso, M.L. People, landscape, and urban heat island: Dynamics among neighborhood social conditions, land cover and surface temperatures. *Landsc. Ecol.* **2016**, *31*, 2507–2515. [CrossRef]

27. Tiner, R.W. Remotely-sensed indicators for monitoring the general condition of "natural habitat" in watersheds: An application for Delaware's Nanticoke River watershed. *Ecol. Indic.* **2004**, *4*, 227–243. [CrossRef]

28. Healey, S.P.; Cohen, W.B.; Yang, Z.Q.; Krankina, O.N. Comparison of tasseled cap-based Landsat data structures for use in forest disturbance detection. *Remote Sens. Environ.* **2005**, *97*, 301–310. [CrossRef]

29. Mildrexler, D.J.; Zhao, M.; Running, S.W. Testing a MODIS global disturbance index across North America. *Remote Sens. Environ.* **2009**, *113*, 2103–2117. [CrossRef]

30. Rhee, J.; Im, J.; Carbone, G.J. Monitoring agricultural drought for arid and humid regions using multi-sensor remote sensing data. *Remote Sens. Environ.* **2010**, *114*, 2875–2887. [CrossRef]

31. Papes, M.; Peterson, A.T.; Powell, G.V.N. Vegetation dynamics and avian seasonal migration: Clues from remotely sensed vegetation indices and ecological niche modeling. *J. Biogeogr.* **2012**, *39*, 652–664. [CrossRef]

32. Gonçalves, J.; Alves, P.; Pôças, I.; Marcos, B.; Sousa-Silva, R.; Lomba, Â.; Honrado, J.P. Exploring the spatiotemporal dynamics of habitat suitability to improve conservation management of a vulnerable plant species. *Biodivers. Conserv.* **2016**, *25*, 2867–2888.

33. Behling, R.; Bochow, M.; Foerster, S.; Roessner, S.; Kaufmann, H. Automated GIS-based derivation of urban ecological indicators using hyperspectral remote sensing and height information. *Ecol. Indic.* **2015**, *48*, 218–234. [CrossRef]

34. Xu, H.Q. A remote sensing urban ecological index and its application. *Acta Ecol. Sin.* **2013**, *33*, 7853–7862.

35. Hu, X.S.; Xu, H.Q. A new remote sensing index for assessing the spatial heterogeneity in urban ecological quality: A case from Fuzhou City, China. *Ecol. Indic.* **2018**, *89*, 11–21. [CrossRef]

36. Song, H.M.; Xue, L. Dynamic monitoring and analysis of ecological environment in Weinan City, Northwest China based on RSEI model. *Chin. J. Appl. Ecol.* **2016**, *27*, 3913–3919.

37. Zhou, M.; Yang, Y. Evaluation of ecological situation in Dongguan city based on remote sensing. *Guangdong Agric. Sci.* **2018**, *45*, 126–134.

38. Yue, H.; Liu, Y.; Li, Y.; Lu, Y. Eco-environmental quality assessment in China's 35 major cities based on remote sensing ecological index. *IEEE Access* **2019**. [CrossRef]

39. Zhang, C.; Xu, H.Q.; Zhang, H.; Tang, F.; Lin, Z.L. Analysis of fractional vegetation cover change and its ecological effect assessment in a typical reddish soil region of Southern China: Changting County, Fujian Province. *J. Nat. Resour.* **2015**, *30*, 917–928.

40. Vermote, E. *MOD09A1 MODIS/Terra surface reflectance 8-Day L3 global 500 m SIN grid V006*; Distributed by NASA EOSDIS LP DAAC; USGS: Sioux Falls, SD, USA, 2015. [CrossRef]

41. Wan, Z.; Hook, S.; Hulley, G. *MOD11A2 MODIS/Terra Land Surface Temperature/Emissivity 8-day L3 Global 1 km SIN grid V006*; Distributed by NASA EOSDIS LP DAAC; USGS: Sioux Falls, SD, USA, 2015. [CrossRef]

42. Kauth, R.J.; Thomas, G.S. The tasseled cap graphic description of the spectral-temporal development of agricultural crops as seen in Landsat. In Proceedings of the Symposium on Machine Processing of Remotely Sensed Data, West Lafayette, IN, USA, 29 June–1 July 1976; pp. 41–51.

43. Huang, C.; Wylie, B.; Yang, L.; Homer, C.; Zylstra, G. Derivation of a tasselled cap transformation based on Landsat 7 at-satellite reflectance. *Int. J. Remote Sens.* **2002**, *23*, 1741–1748. [CrossRef]

44. Crist, E.P.; Cicone, R.C. A physically-based transformation of Thematic Mapper data—The TM Tasseled Cap. *IEEE Trans. Geosci. Remote Sens.* **1984**, *22*, 256–263. [CrossRef]

45. Lobser, S.E.; Cohen, W.B. MODIS tasselled cap: Land cover characteristics expressed through transformed MODIS data. *Int. J. Remote Sens.* **2007**, *28*, 5079–5101. [CrossRef]

46. Xu, H.Q. A new index for delineating built-up land features in satellite imagery. *Int. J. Remote Sens.* **2008**, *29*, 4269–4276. [CrossRef]

47. Weng, Q.; Fu, P.; Gao, F. Generating daily land surface temperature at Landsat resolution by fusing Landsat and MODIS data. *Remote Sens. Environ.* **2014**, *145*, 55–67. [CrossRef]

48. Xu, H.Q. Dynamic of soil exposure intensity and its effect on thermal environment change. *Int. J. Climatol.* **2014**, *34*, 902–910. [CrossRef]

49. MEP. *Technical Criterion for Ecosystem Status Evaluation*; Trial Version; Environmental Science Press: Beijing, China, 2006.

50. Wang, S.Y.; Zhang, X.X.; Zhu, T.; Yang, W.; Zhao, J.Y. Assessment of ecological environment quality in the Changbai Mountain Nature Reserve based on remote sensing technology. *Prog. Geogr.* **2016**, *35*, 1269–1278.

51. Liu, Y.; Yue, H.; Meng, J.; Zhang, F.; Cui, Q. Ecological environment assessment for the main cities along the Silk Road Economic Belt (China section) based on remote sensing. *Admin. Tech. Environ. Monit.* **2018**, *30*, 35–39.

52. Zhang, X.; Liu, X.; Zhao, Z.; Ma, Y.; Yang, Y. Dynamic monitoring of ecology and environment in the agro-pastral ecotone based on remote sensing: A case of Yanchi County in Ningxia Hui Autonomous Region. *Arid. Land. Geogr.* **2017**, *40*, 1070–1078.

53. Jiang, C.; Wu, L.; Liu, D.; Wang, S. Dynamic monitoring of eco-environmental quality by remote sensing in arid desert area: Taking the Gurbantunggut Desert China as an example. *Chin. J. Appl. Ecol.* **2019**, *30*, 277–284.

54. Hwang, T.; Song, C.; Bolstad, P.V.; Band, L.E. Downscaling real-time vegetation dynamics by fusing multi-temporal MODIS and Landsat NDVI in topographically complex terrain. *Remote Sens. Environ.* **2011**, *115*, 2499–2512. [CrossRef]

55. Agam, N.; Kustas, W.; Anderson, M.; Li, F.; Neale, C. A vegetation index based technique for spatial sharpening of thermal imagery. *Remote Sens. Environ.* **2007**, *107*, 545–558. [CrossRef]

56. Xian, G.; Homer, C.; Fry, J. Updating the 2001 National Land Cover Database land cover classification to 2006 by using Landsat imagery change detection methods. *Remote Sens. Environ.* **2009**, *113*, 1133–1147. [CrossRef]

57. Yu, W.; Zhou, W.; Qian, Y.; Yan, J. A new approach for land cover classification and change analysis: Integrating backdating and an object-based method. *Remote Sens. Environ.* **2016**, *177*, 37–47. [CrossRef]

58. Dewi, R.S.; Bijker, W.; Stein, A. Change vector analysis to monitor the changes in fuzzy shorelines. *Remote Sens.* **2017**, *9*, 147. [CrossRef]

59. Morisette, J.T.; Khorram, S. Accuracy assessment curves for satellite-based change detection. *Photogramm. Eng. Remote. Sens.* **2000**, *66*, 875–880.

60. Zhu, Z. Change detection using Landsat time series: A review of frequencies, preprocessing, algorithms, and applications. *ISPRS J. Photogramm.* **2017**, *130*, 370–384. [CrossRef]

61. Massey, F.J. The Kolmogorov-Smirnov test for goodness of fit. *J. Am. Stat. Assoc.* **1951**, *46*, 68–78. [CrossRef]

62. Gilbert, R.O. *Statistical Methods for Environmental Pollution Monitoring*; Wiley: New York, NY, USA, 1987; p. 320.

63. Theil, H. A rank-invariant method of linear and polynomial regression analysis. *Nederlandse Akademie Wetenchappen Ser. A.* **1950**, *53*, 386–392.

64. Sen, P.K. Estimates of the regression coefficient based on Kendall's tau. *J. Am. Stat. Assoc.* **1968**, *63*, 1379–1389. [CrossRef]

65. Li, X.; Zhou, Y.; Zhu, Z.; Liang, L.; Yu, B.; Cao, W. Mapping annual urban dynamics (1985–2015) using time series of Landsat Data. *Remote Sens. Environ.* **2018**, *216*, 674–683. [CrossRef]

66. Zhang, J.; Yang, Y. Remote sensing evaluation on the change of ecological status of Pearl River delta urban agglomeration. *J. Northwest For. Univ.* **2019**, *34*, 184–191.

67. Dale, V.H.; Beyeler, S.C. Challenges in the development and use of ecological indicators. *Ecol. Indic.* **2001**, *1*, 3–10. [CrossRef]

68. Niemeijer, D.; de Groot, R.S. A conceptual framework for selecting environmental indicator sets. *Ecol. Indic.* **2008**, *8*, 14–25. [CrossRef]

69. Hu, X.; Xu, H. A new remote sensing index based on the pressure-state-response framework to assess regional ecological change. *Environ. Sci. Pollut. Res.* **2019**, *26*, 5381–5393. [CrossRef] [PubMed]

70. OECD. *OECD Environmental Indicators: Towards Sustainable Development*; Organisation for Economic Cooperation and Development: Paris, France, 2001; 155p.

71. Hughey, K.F.D.; Cullen, R.; Kerr, G.N.; Cook, A.J. Application of the pressure–state–response framework to perceptions reporting of the state of the New Zealand environment. *J. Environ. Manag.* **2004**, *70*, 85–93. [CrossRef]

72. Cheng, J.N.; Zhao, G.X.; Li, H. Dynamic changes and evaluation of land ecological environment status based on RS and GIS technique. *Trans. CSAE* **2008**, *24*, 83–88.

73. Meng, Y.; Zhao, G.X. Ecological environment condition evaluation of estuarine area based on quantitative remote sensing—A case study in Kenli County. *Chin. Environ. Sci.* **2009**, *29*, 163–167.

74. Wen, X.L.; Lin, Z.F.; Tang, F. Remote sensing analysis of ecological change caused by construction of the new island city: Pingtan Comprehensive Experimental Zone, Fujian Province. *Chin. J. Appl. Ecol.* **2015**, *26*, 541–547.

75. Xu, H.Q.; Zhang, H. Ecological response to urban expansion in an island city: Xiamen, southeastern China. *Sci. Geogr. Sin.* **2015**, *35*, 867–872.

76. Shi, T.T.; Xu, H.Q.; Tang, F. Built-up land change and its impact on ecological quality in a fast-growing economic zone: Jinjiang County, Fujian Province, China. *Chin. J. Appl. Ecol.* **2017**, *28*, 1317–1325.

77. Wang, M.Y.; Xu, H.Q. Temporal and spatial changes of urban impervious increase and its influence on urban ecological quality: A comparison between Shanghai and New York. *Chin. J. Appl. Ecol.* **2018**, *29*, 3735–3746.

78. Zhang, H.; Du, P.J.; Luo, J.Q.; Li, E.Z. A RSEI-based analysis on the ecological changes of Nanjing city. *Geospat. Inform.* **2017**, *15*, 58–62.

79. Peng, L.; Zhang, J.; Liang, E.; Hu, M. Evaluation of natural ecological environment change in Manasi River Basin based on RSEI. *J. Shihezi Univ. Nat. Sci.* **2017**, *35*, 506–512.

80. Li, Q.; Wang, Z.; Qui, J.; Yang, G.; Yang, Y.; Liang, G. Study on the classification of ecological environmental quality index RSEI in Aksu city based on TM data. *Tianjin Agric. Sci.* **2018**, *24*, 63–67.